Journal of Chromatography B, 878 (2010) 933–941

Contents lists available at ScienceDirect

Journal of Chromatography B

journal homepage: www.elsevier.com/locate/chromb

New monolith technology for automated anion-exchange purification of nucleic acids

J.R. Thayer*, K.J. Flook, A. Woodruff, S. Rao, C.A. Pohl

Dionex Corporation, 445 Lakeside Drive, Sunnyvale, CA 94085, United States

ARTICLE INFO

Article history:
Received 3 November 2009
Accepted 21 January 2010
Available online 29 January 2010

Keywords:
Nucleic acid purification
Hybrid monolith
Anion-exchange HPLC
Oligonucleotide linkage isomers
Phosphorothioate diastereoisomers
Oligonucleotide desalting
ESI-MS
DNAPac
DNASwift

ABSTRACT

Synthetic nucleic acid analysis often employs pellicular anion-exchange (AE) chromatography because it supports very high efficiency separations while offering means to control secondary structure, retention and resolution by readily modifiable chromatographic conditions. However, these pellicular anion-exchange (pAE) phases do not offer capacity sufficient for lab-scale oligonucleotide (ON) purification. In contrast, monolithic phases produce fast separations at capacities exceeding their pellicular counterparts, but do not exhibit capacities typical of fully porous, bead-based, anion-exchangers. In order to further increase monolith capacity and obtain the selectivity and mass transfer characteristics of pellicular phases, a surface-functionalized monolith was coated with pAE nanobeads (latexes) usually employed on the pellicular DNAPac phase. The nanobead-coated monolith exhibited chromatographic behaviors typical of polymer AE phases. Based on this observation the monolithic substrate surface porosity and latex diameters were co-optimized to produce a hybrid monolith harboring capacity similar to that of fully porous bead-based phases and peak shape approaching that of the pAE phases. We tested the hybrid monolith on a variety of previously developed pAE capabilities including control of ON selectivity, resolution of derivatized ONs, the ability to resolve RNA ONs harboring aberrant linkages at different positions in a single sequence and separation of phosphorothioate diastereoisomers. We compared the yield and purity of an 8 mg ON sample purified on both the new hybrid monolith and a benchmark AE column based on fully porous monodisperse beads. This comparison included an assessment of the relative selectivities of both columns. Finally, we demonstrated the ability to couple AE ON separations with ESI-MS using an automated desalting protocol. This protocol is also useful for preparing ONs for other assays, such as enzyme treatments, that may be sensitive to high salt levels.

1. Introduction

Oligonucleotides (ONs) are used as primers and probes for PCR and related amplification techniques as well as diagnostic and therapeutic agents [1–3]. Therapeutic ONs must be resistant to nucleolytic attack, as they are administered in a manner exposing them to metabolically active bodily fluids. To protect them from these activities, chemical modifications are applied to the ON, depending on the specific therapeutic approach [4–7]. While improvements to ON synthesis can often provide sufficient purity for use as amplification probes, ONs intended for diagnostic and therapeutic applications must be purified and thoroughly characterized after synthesis [8]. Such purifications often employ anion-exchange (AE) chromatography, because unlike gel electrophoretic and reversed-phase separations, the AE approach offers several powerful mechanisms for control of retention and selectivity [8–10]. In the initial stages of development, small-scale samples up to 200 μg may be purified for early screenings, but milligram quantities are needed for bioanalysis of promising candidates. While very high purities can be obtained using high resolution non-porous anion-exchangers, these phases typically harbor capacities too limited for lab-scale purification, but have occasionally been used [11]. Porous anion-exchangers provide sufficient capacity for lab-scale purifications, but typically exhibit very low throughput, or compromised resolution due to slow mass transport. In one example a 90-min gradient was used to resolve a common 14 base oligo with a single phosphorodithioate, a single phosphoromonothioate and athioate forms [7]. Preparation of a very thin ion-exchange surface on a non-porous resin overcomes the limitation of mass transport kinetics, producing high efficiency, high-resolution separations [12], and supports fast separation of oligonucleotides and their metabolites from serum for metabolic studies [13]. One approach to that route consists of applying 50–400 nm ion-exchange latex "nanobeads" to the surface of a non-porous substrate [14]. By controlling the nanobead chemistry [15], permeability may be engineered so that the entire bead

* Corresponding author. Tel.: +1 408 481 4466.
E-mail address: jim.thayer@dionex.com (J.R. Thayer).

1570-0232/$ – see front matter © 2010 Elsevier B.V. All rights reserved.
doi:10.1016/j.jchromb.2010.01.030

volume becomes accessible to ON analytes. In such cases, increasing the nanobead diameter will also increase the ion-exchange capacity.

Monoliths are continuous polymers with through pores that are polymerized into columns for chromatographic uses [16]. For nearly two decades monoliths have enjoyed increasing interest for the separation of biomolecules including oligonucleotides and nucleic acids [17,18]. After surface-functionalization, monolithic disks have been used for ion-exchange based nucleic acid separations, but when produced in the disk format, relatively broad peaks were observed [19]. More recently latex-coated monoliths were reported for the separation of small ions [20,21] and sugars [22], but are not commercially available. Selection of monomers, porogens and polymerization conditions during synthesis permits independent adjustment of surface area and porosity [23,24]. Hence, the monolith may be optimized to accommodate a specific nanobead size and chemistry. Surface modification and nanobead attachment should produce capacity similar to that of fully porous beads, and efficiency, selectivity, and stability similar to that of pellicular anion-exchangers. In light of these considerations, a high-capacity, high resolution AE phase designed for nucleic acid chromatography would find utility for purification of medically important ONs for preclinical screening. In order to successfully perform purifications on therapeutic ONs, a purification column must resolve isomers arising from these ON modifications. Pellicular anion-exchangers have been shown to resolve many of these including: RNA [8], 2′,5′-linkages [25,26], phosphoramidate-linked RNA [4,27], phosphorothioate-linked ONs [28,29], DNA containing a variety of modified bases [10], DNA containing intrastrand cross-links [30], 1-methyl- and 6-methyl-adenine containing oligos [31], cisplatin-modified DNA [32,33], 2′-cyanoethoxymethyl-protected RNA [6], DNA containing a universal base analog (5-nitroindol) [34], and oligonucleotides harboring phosphorothioate diastereoisomers [35]. If these capabilities derive from the pellicular coating, the latexed monolith would constitute a significant advance for purification of clinically important nucleic acids. In this report we describe a new pellicular AE monolith, the DNASwift™ SAX-1S, its characteristics and application for lab-scale oligonucleotide purification and post-purification desalting for further analyses.

2. Materials and methods

2.1. Chemicals

Sodium chloride, Trizma base (Tris), 2-amino-2-methyl-1-propanol (AMP) and diisopropylamine (DIPA), were obtained from Sigma. Phosphoric acid and sodium phosphate were obtained from E.M. Science. Methane sulfonic acid (MSA) and ammonium formate were from Fluka. Sodium perchlorate was obtained from GFS or Fluka. Methanol and acetonitrile were from Honeywell (Burdick and Jackson). Oligonucleotides were obtained from Life Technologies, Integrated DNA Technologies, or Sigma-GenoSys. Deionized water was prepared using a Millipore Milli-Q Plus deionizing system to prepare 18 Meg-Ohm/cm water.

2.2. Chromatographic equipment

Dionex ICS3000® and UltiMate®-3000 Titanium chromatography systems were controlled by Chromeleon® Chromatography Management Software. Fractionation was accomplished using the fraction-collecting option of the WPS-3000 autosampler (Dionex). Short silica reversed-phase columns were from Dionex (Acclaim PA-2 C18, 3 μm, 4.6 mm × 50 mm). A ProSwift® SCX monolith (4.6 mm × 50 mm, Dionex) was used for the initial evaluation of latex coating. For this study, stationary phase volumes from packed bed and monolithic columns are compared. Hence, column volume (CV) denotes the volume occupied by the stationary phase (i.e., the complete internal column volume). Purification of nucleic acids was performed on a DNASwift™ SAX-1S monolith (5 mm × 150 mm, Dionex, CV = 2.5 mL), or a Mono-Q HR 5/5 column (5 mm × 50 mm, GE Healthcare, CV = 1 mL). Analysis of the purified components employed a DNAPac PA200 column (2 mm × 250 mm, Dionex, CV = 0.79 mL). Chromatographic conditions for the various experiments are described in the legends to the accompanying figures.

In general, gradient elution of ON samples is employed, and we used a previously described eluent system [9,25]. In brief, this system consists of 4 eluents: (A) deionized H_2O, (B) 0.2 M NaOH, (C) 0.2 M Tris, 0.2 M AMP and 0.2 M DIPA adjusted to pH 7.2 with MSA, and (D) either 0.33 M $NaClO_4$ or 1.25 M NaCl. Adjustment of the eluent pH was accomplished by proportioning eluents B and C to a total of 20%, using a proportion vs pH calibration. Since this eluent includes several buffers, we prepare the calibration curve in Microsoft Excel using a sixth-order polynomial equation. With this system 20% eluent C will produce pH 7 and 20% eluent B will produce pH 12.6. This eluent system employs constant proportions of eluent B and C to maintain the pH, while eluents A and D are used to produce a salt gradient for ON elution.

2.3. Oligonucleotide purification, desalting and assay

Cartridge-deprotected ONs were purified on a Dionex DNASwift SAX-1S 5 mm × 150 mm monolith as described in the figures. The monolith volume was 2.5 mL and gradients used were dependent

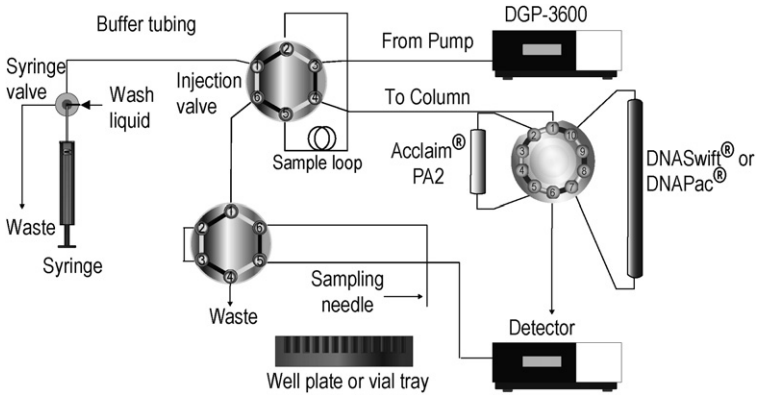

Scheme 1. An inert 4-eluent HPLC system with a fraction-collecting autosampler as used for purification, desalting and analysis of oligonucleotides.

on the length and composition of the oligonucleotides. Purified fractions were analyzed on a 2 mm × 250 mm DNAPac PA200 at various temperatures and pH values (as indicated), using linear or curved gradients [9,36] at 300 μL/min. Using a Dionex WPS-3000 TBFC fraction collecting autosampler, we configured a system for automatic purification and desalting (Scheme 1). The system employed a quaternary gradient pump with two eluents for ion-exchange, and two eluents for reversed-phase. This system also included a WPS autosampler, a column oven with column switching valves and an absorbance detector. As Step 1, eluents 1 and 2 (buffered solutions containing different concentrations of salt, e.g. 20 mM Tris–HCl, pH 8 with 0, or 1.25 M NaCl) were used to purify the oligonucleotide on a DNASwift SAX-1S monolith (column selection valve in the 1–10 position). As the peaks eluted they were collected into vials or a 96-well plate in the autosampler. Upon completion of the purification(s), a second step was initiated: The column switching valve was set to the 1–2 position to direct the pumped eluents to the Acclaim PA-2 reversed-phase cartridge. Here, eluent 3 (the reversed-phase eluent consisting of 20 mM ammonium formate pH 6 without solvent) was applied to equilibrate the cartridge. The samples collected from the DNASwift, and containing high salt concentrations were injected onto the PA-2 cartridge where oligonucleotides bound, but salt washed through. Salt elution was monitored using a Dionex ED50 detector with a conductivity cell. After the salt had washed out, the ONs were eluted from the PA-2 cartridge using a short step to eluent 4 (the reversed-phase eluent, containing 40% MeOH). The desalted ON eluted, and was collected for later MS analysis, or diverted directly into a coupled ESI-MS for immediate assay. In this study, the samples were collected, then dried by centrifugal evaporation and stored at −20 °C until resuspended for use.

2.4. Nanobead coating of the prototype monolith

Using a ProSwift SCX-1S (4.6 mm × 50 mm) monolith column a dilute aqueous solution of the DNAPac PA200 latex was pumped through the column until break through was observed. The method is a modification of previously published procedures [12,15,21,22].

2.5. Sample overloading comparison of the DNASwift and Mono-Q columns

To prepare the appropriate method for this comparison, we selected a 25-base ON, and optimized the gradient to elute an 8 μg sample of this ON just prior to the column wash step for each of the two columns. Because very high sample loads result in band broadening and sample elution significantly before the beginning of the sample peak at analytical loads, we began fraction collection several CV earlier than the elution position of the 8 μg sample. Specifically, we programmed the following gradient for each column: equilibrate at 10% of the final eluent proportion; step from 10 to 70% of the final eluent proportion in 0.7 CV; and perform gradient elution from 70 to 100% of the final eluent concentration in 12 CV. During this gradient, thirty 0.2 CV fractions were collected, starting 6 CV (30 fractions × 0.2 CV) before the end of the 8 μg sample elution position. Dilutions of the collected fractions were prepared with deionized H_2O and analyzed on a DNAPac PA200 to evaluate their purity and to calculate sample recovery. The gradient for the DNAPac analysis was 50–150 mM $NaClO_4$ in 12 min using curved gradient 4 (see Ref. [9] for the gradient number equation). The eluent was buffered to pH 7 with 20 mM Tris–HCl, flow was 300 μL/min, and the temperature was 60 °C. The yield of collected ON was calculated based on the known dilutions, injection volumes, fraction volumes and peak areas, as compared to the known amount loaded (8.25 mg) by full loop injection onto each column.

2.6. Selectivity assessment

Five oligonucleotides that share a common 23-base sequence were selected as test probes. Dx-80, -83, and -85 (Table 1) are 25-mers with different 3′ and/or 5′ terminal bases. Dx-86, and -87 (Table 1, both 24mers), harbor either a 5′C or a 3′A. These 24-mers were selected as "$n-1$" probes to monitor the ability of each column to resolve them from the three different 25-base oligos. A steep linear gradient of 200–1000 mM NaCl in 9 CV was employed to compare the relative selectivities. Chromatography of each ON was performed at nine different pH values and the retention time and

Table 1
Oligonucleotides used for this study. For the eGFP antisense strands, the positions of intentionally introduced 2′,5′-linkages are highlighted by underlines and boldface type.

Name	Sequences	Figures	Forms
AR25:	5′-GGG ATG CAG ATC ACT TTC CG -3′	Figs. 1–3	DNA
Dx78:	5′-CTG CTT GTA GGA TCT TTA AAG ACG T-3′	Fig. 5	DNA
DX80:	5′-ATG ATT GTA GGT TCT CTA ACG CTG A-3′	Tables 2 and 3	DNA
Dx83:	5′-CTG ATT GTA GGT TCT CTA ACG CTG T-3′	Fig. 10, Tables 2 and 3	DNA
Dx85:	5′-CTG ATT GTA GGT TCT CTA ACG CTG G -3′	Tables 2 and 3	DNA
Dx86:	5′- TG ATT GTA GGT TCT CTA ACG CTG A-3′	Tables 2 and 3	DNA
Dx87:	5′-CTG ATT GTA GGT TCT CTA ACG CTG-3′	Tables 2 and 3	DNA
Dx88:	5′- G ATT GTA GGT TCT CTA ACG CTG A-3′	Fig. 4	DNA
Dx89:	5′- TG ATT GTA GGT TCT CTA ACG CTG-3′	Fig. 4	DNA
Dio1:[a]	5′-AUG AAC UUC AGG GUC AGC UUG -3′	Fig. 6	RNA
Dio2:	5′-**A**UG AAC UUC AGG GUC AGC UUG -3′	Fig. 6	RNA
Dio3:	5′-**AU**G AAC UUC AGG GUC AGC UUG -3′	Fig. 6	RNA
Dio4:	5′-**AUG** AAC UUC AGG GUC AGC UUG -3′	Fig. 6	RNA
Dio5:	5′-AUG AAC UUC **A**GG GUC AGC UUG -3′	Fig. 6	RNA
Dio6:	5′-AUG AAC UUC **AG**G GUC AGC UUG -3′	Fig. 6	RNA
Dio7:	5′-AUG AAC UUC **AG** GUC AGC UUG -3′	Fig. 6	RNA
Dio8:	5′-AUG A**A**C UUC AGG GUC AGC UUG -3′	Fig. 6	RNA
Dio9:	5′-AUG AAC UUC AGG GU**C** AGC UUG -3′	Fig. 6	RNA
Dio10:	5′-AUG AAC UUC AGG GUC AGC U**U**G -3′	Fig. 6	RNA
Dio11:	5′-AUG AAC UUC AGG GUC AG**C** U**U**G -3′	Figs. 6, 8 and 9	RNA
Dio12:	5′-AUG AAC UUC AGG GUC AGC **UU**G -3′	Fig. 6	RNA
eGFP:[b]	5′-AGC UGA CCC UGA AGU UCA UdCdT	Fig. 7	RNA and DNA
eGFP:	5′-AGC UGA_S CCC UGA AG_SU UCA UdCdT	Fig. 7	RNA and DNA

[a] Bases that are Emboldened, and underlined in Dio-1 through Dio-12 have 2′–5′ linkages.
[b] Sequences with subscript "S" indicate the positions of phosphorothioate linkages.

flow rate were used to determine the elution differences (expressed in μL) for each condition. In order to allow direct comparison, these retention difference values were converted to CV. For this comparison, the selectivity values were tabulated, with the frequency of superior values for each column. Another parameter we considered is the relative frequency of "negative selectivity". Selectivities with a negative sign indicate elution of the 24mer after the 25mer. Where separation of full length ONs from "$n-1$" failure sequences is considered, an oligo pair with a zero or negative selectivity will generally not allow discrimination of the shorter oligo. As with the relative selectivity data, the frequency of zero, and negative selectivity values was summed for comparison. Note that if negative selectivities are observed, options for manipulating the eluent conditions to reverse the elution order inversion are important to demonstrate.

3. Results and discussion

3.1. Effect of latex coating

Since previously reported latex-coated monoliths were not designed for use with oligonucleotides, we confirmed that chromatographic performance of a latex-coated monolith would approach that of a high efficiency non-porous phase. A 20-base partially tritylated oligonucleotide was analyzed to compare the latex-coated monolith with a porous bead-based column (Mono-Q) and a pellicular anion exchanger (DNAPac). In Fig. 1, a 25 μg sample was injected on each column, and eluted using similar gradients. Due to the pressure limit imposed by the porous phase, we ran the Mono-Q column at a lower flow rate (and thus reduced linear velocity). The pellicular DNAPac column exhibited peak width at half-height ($PW^{1/2}$) values of 88 and 108 μl for the detritylated and tritylated forms, respectively. The porous anion-exchanger exhibited $PW^{1/2}$ values of 205 and 475 μL respectively, even at the lower flow rate where the effect of diffusive mass transfer was reduced. In contrast, application of the DNAPac PA200 latex to the monolith surface resulted in $PW^{1/2}$ values of 106 and 137 μL for the detritylated and tritylated 20-mer, respectively. Thus, the latexed monolith produced $PW^{1/2}$ values 20 and 27% greater than those of the non-porous DNAPac column (detritylated and tritylated, respectively), but still only 52 and 29% of the $PW^{1/2}$ of the porous bead-based column (detritylated and tritylated full-length oligos, respectively). It should also be noted that the peak for the tritylated ON in the Mono Q separation exhibited significant tailing. This is likely due to unwanted hydrophobic interactions, and was not observed for either latexed phase. We suspect that most hydrophobic interactions between the ON and the support may be shielded by the latex coating. Unshielded interactions on either phase may be controlled by addition of 5–10% solvent (e.g., methanol or acetonitrile) to the eluents (unpublished observations).

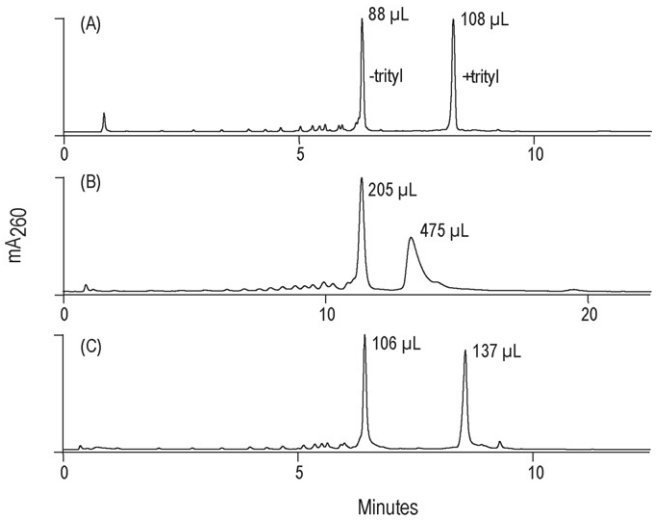

Fig. 1. Comparison of relative peak width ($PW^{1/2}$), and selectivity of a 4 mm × 250 mm DNAPac PA200 (A), a 5 mm × 50 mm Mono-Q (GE/Healthcare), (B) and a 4.6 mm × 50 mm ProSwift SCX monolith coated with the DNAPac nanobeads (C). Gradient: 100–800 mM NaCl in 15 mL at 30 °C and pH 8. Peak labels indicate $PW^{1/2}$ (in μL).

3.2. Comparison of the DNASwift SAX-1S to the Mono-Q

Keeping the DNAPac latex chemistry intact, we optimized the latex size, and monolith porosity/surface area. Our overall goals included increased loading capacity, improved resolution, and minimal purification time. We found that capacity could be improved by applying anion-exchange nanobeads (latex), and further improved by increasing the diameter of the latex. However, this required control of the monolith surface area and pore structure to accommodate the larger latexes. Hence, this goal required assessment of different monomer and porogen systems, and optimization of these parameters to provide a high capacity phase. Resolution for purification columns is a function of selectivity and substrate efficiency. We previously optimized latexes for oligonucleotide separations for the DNAPac PA100 and PA200 columns, so we employed that chemistry altering only the latex size for capacity improvement. Nucleic acid purification protocols historically required elution gradients, so we employed measurements of *peak width* to assess phase efficiency. For this goal we re-optimized the monolith pore structure to support mass transfer primarily by convection rather than diffusion, as that improved efficiency.

Preparation of a hybrid phase offering minimal purification time (improved throughput) requires a pressure stable substrate. Hence, we used a high cross-link monolith with relatively high surface area (for latex attachment) and fairly wide pores to accommodate the attached latex without undue pressure. Preparation of such a monolithic substrate required further optimization of the monomer, spacer, and porogen systems to support operation at pH values between 6 and 12.4, for optimal nucleic acid hydrogen-bonding and selectivity control. This required alteration of the monomer to that employed with the DNAPac PA200 latex (that monomer and its pH stability characteristics are described in Ref. [9]). Finally, small latexes support convection-dominated mass transfer, but increasing their size also shifts mass transfer toward diffusion. This required further optimization of latex diameter, monolith surface area and monolith pore-structure to prepare the desired anion-exchange phase to accomplish these goals. The final monolith modal pore size was 3 μm.

Fig. 2 compares the $PW^{1/2}$ as a function of the amount of sample loaded on the DNAPac PA200, Mono-Q and DNASwift columns. Because these columns have different diameters and lengths (and hence different column volumes), the gradients used to generate this data were designed to deliver the same linear velocity (flow/cross sectional area), and to apply the gradient across the same number of CV (as defined in Section 2.2). We expressed the $PW^{1/2}$ results as percent of column volume (%CV) to normalize the data for comparison. The DNAPac PA200 column exhibited very narrow peak width at the lowest sample loads (i.e. 0.5 μg), but also overloaded at very low sample amounts (25–50 μg). Conversely, the porous bead-based Mono-Q showed relatively high $PW^{1/2}$ values at the lowest sample concentrations, but appeared capable of handling oligonucleotide injections up to 1.1 mg with comparatively little change in chromatographic performance. The DNASwift SAX-1S anion-exchange monolith exhibited intermediate $PW^{1/2}$ values at the lowest sample concentrations, and like the Mono-Q, accommodated increased loads with comparatively little change

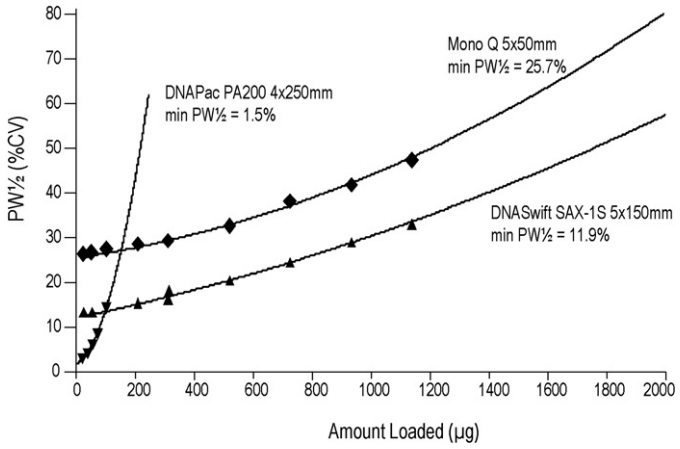

Fig. 2. Comparison of the sensitivity to sample load of a 4 mm × 250 mm DNAPac PA200, a 5 mm × 50 mm Mono-Q (GE/Healthcare) and a 5 mm × 150 mm DNASwift SAX-1S. Gradient: 100–800 mM NaCl in 21.5 column volumes (CV) at a linear velocity of 1.5 mm/s. Column volumes are: DNAPac PA200 (3.1 mL), Mono-Q (0.98 mL), DNASwift SAX-1S (2.5 mL).

in chromatographic performance. In this example, the monolith exhibited a $PW^{1/2}$ value at 1.1 mg comparable to that of the Mono-Q at 0.5 mg, suggesting the capability of sample loads over twice that of the Mono-Q for equivalent purifications. The regression lines for each column's data in Fig. 2 are second-order polynomials. The intercept at zero µg of sample indicates the theoretically optimal $PW^{1/2}$ values. They were 1.5% CV for the DNAPac non-porous column, 11.9% CV for the monolith and 25.7% CV for the Mono-Q. An advantage of the monolith approach is higher pressure stability and increased permeability, allowing flow up to 3 mL/min, and at pressures up to 1500 psi (data not shown).

3.3. Temperature effects

A characteristic of oligonucleotide chromatography on anion-exchangers is increased retention and resolution at increasing temperatures. To verify that the monolithic phase presents primarily anion-exchange functionality, we evaluated the effect of temperature on retention and resolution of a 20-base ON.

Fig. 3 shows that increasing temperature during gradient elution chromatography on the DNASwift monolith increased retention, and decreased $PW^{1/2}$ (improved resolution), verifying anion-exchange behavior.

3.4. Selectivity control

The DNASwift monolith performs well in the tests described above. However, critical analysis requires demonstration of performance similar to the pellicular anion-exchanger for a variety of useful applications. In order to verify that the DNASwift monolith maintains the chromatographic selectivity attributes of the DNAPac columns we examined the pellicular monolith for three critical capabilities previously observed for the DNAPac columns: (1) The ability to reverse elution order of related ONs by modulating the pH and salt-form (selectivity control); (2) the resolution of fluorophore derivatized ONs from their unlabeled counterparts, and (3) the ability to resolve isobaric aberrant linkage isomers in RNA [25,26].

3.4.1. Selectivity inversion

Fig. 4A shows the effect of increasing pH on the retention and resolution of a pair of 23-base ONs using the DNASwift Monolith. Changes in pH result in ionization of tautomeric oxygens in G, T and U bases, thus increasing their net charge and retention by AE

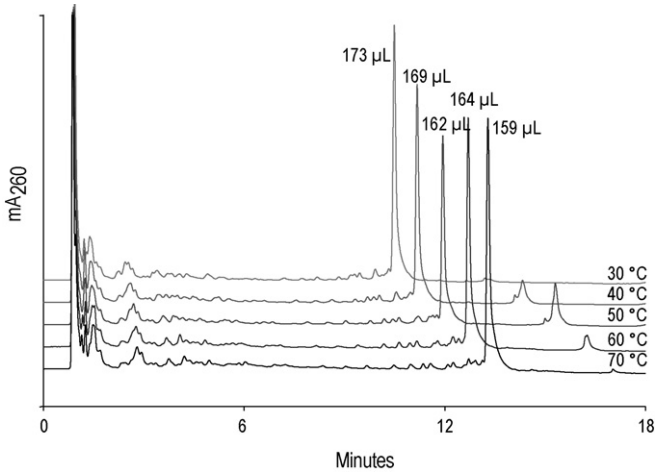

Fig. 3. Effect of temperature on oligonucleotide retention and resolution on the DNASwift SAX-1S. Sample: 8 µg of a 20-base oligonucleotide (see Table 1 for sequence). Elution: 100–800 mM NaCl in 15 min at 1.77 mL/min (linear velocity = 1.5 mm/s), at temperatures from 30 to 70 °C and at pH 8. Peak labels indicate $PW^{1/2}$ (in µL).

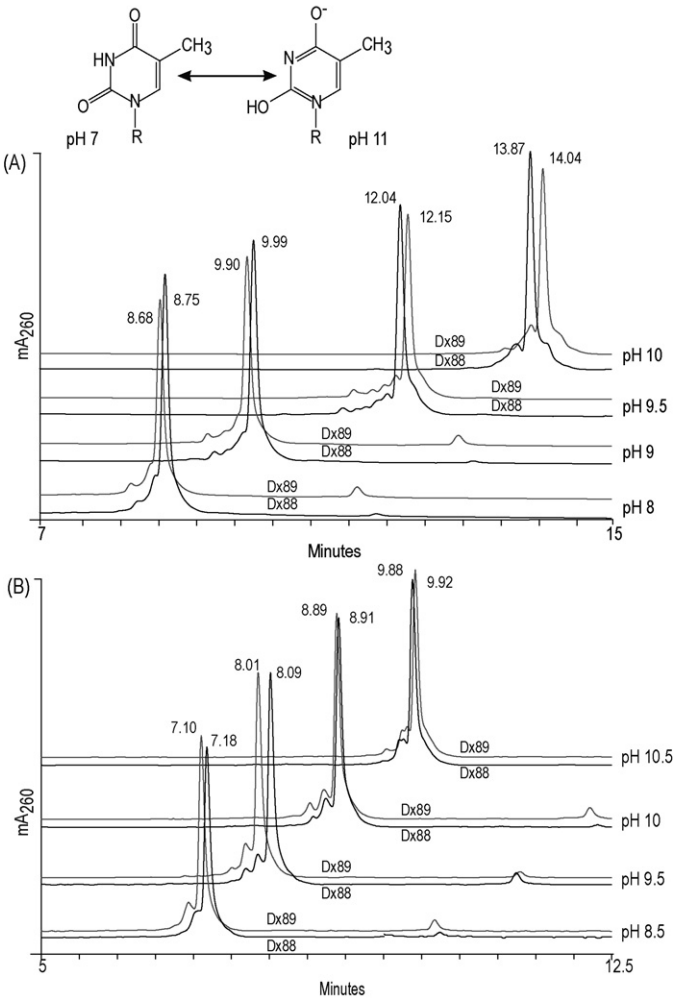

Fig. 4. (A) Effect of pH on DNASwift retention and selectivity using NaCl. Gradient: 200–1000 mM NaCl in 10 CV at 30 °C and 1.5 mL/min using pH values from 8 to 10. Samples: 20 µL of Dx88 and Dx89 (see Table 1 for sequences). (B) Effect of pH on DNASwift retention and selectivity using $NaClO_4$. Samples as in (A), Gradient: 10–195 mM $NaClO_4$ in 12 CV at 2.0 mL/min and at 30 °C, using pH values from 8.5 to 10.5. Peak labels indicate retention time (min).

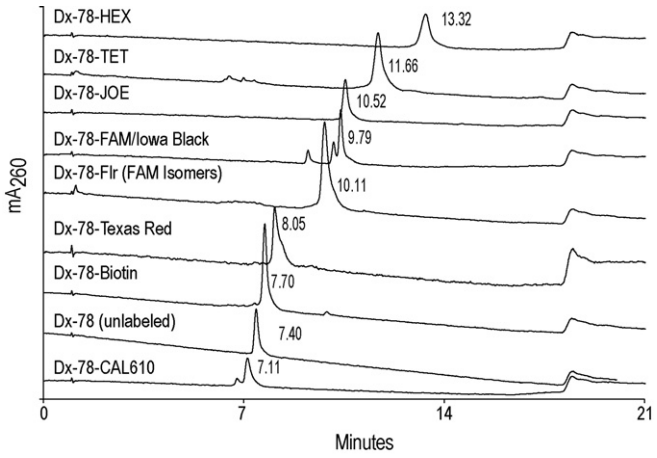

Fig. 5. Resolution of derivatized from an underivatized parent sequence on the DNASwift column. Gradient: 200–1000 mM NaCl in 9 CV at pH 7 and 30 °C. Samples: Dx78 (see Table 1 for sequence) 2.8–3.5 μg per injection. Peak labels indicate retention time (min).

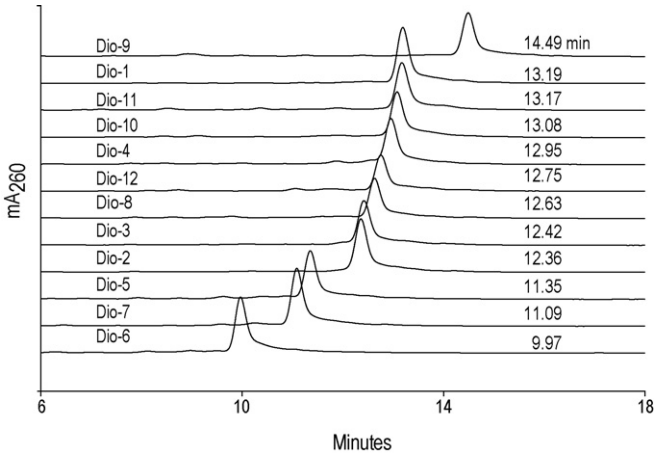

Fig. 6. Resolution of RNA linkage isomers on the DNASwift SAX-1S Monolith. Gradient: 325–575 mM NaCl in 10 CV, at 1.5 mL/min, 30 °C and pH 7. Samples: Dio-1 through Dio-12 (see Table 1). Peak labels indicate retention time (min).

chromatography [9,10]. These oligos differ only in that Dx88 has a 3′ adenosine absent in DX89, while Dx89 harbors a 5′ thymidine absent in Dx88 (all intervening bases are identical, see Table 1). In Fig. 4A, sodium chloride is the eluent. Retention increases are not the same for both ONs as each has a different complement of T and G due to their different 5′ and 3′ bases. Due to these differences the elution order (selectivity) is also influenced by pH. In this case the best resolution was at pH 10. Although the order of elution was reversed between pH 8 and 10, the two ONs were not well resolved at the lower pH.

Fig. 4B shows the same separation, but using $NaClO_4$ as eluent. In this example Dx89 elutes first, and is adequately resolved from Dx88 at pH 9.5, indicating the effect expected from prior DNAPac studies (unpublished observations).

3.4.2. Resolution of derivatized from an underivatized parent sequence

Fig. 5 shows the ability to differentially retain a parent ON (Dx78 see Table 1) from its derivatives where the added moiety was Biotin, or common dyes including Fluorescein (Flr) and TET (5′-linked), and Cal610, JOE, Texas Red, and Hex (3′-linked). In addition, the ON dually labeled with FAM and Iowa Black quencher is resolved from the parent Dx-78, and from the ON labeled with the FAM mixed isomers (Flr). Under these conditions, each ON eluted at a different time offering the opportunity to purify each from the others. This experiment employed a steep (survey) gradient of 200–1000 mM NaCl in 15 min at 1.5 mL/min. Improved resolution may be obtained for each derivative using a shallower gradient, such as 300–850 mM in 15 min, and peak shape may be improved by addition of 5–10% acetonitrile as suggested earlier.

3.4.3. Resolution of RNA samples differing only in the position of aberrant 2′,5′-linkages in the common sequence

Fig. 6 demonstrates that, like the DNAPac column [25,26], the DNASwift monolith resolves several of the aberrantly linked RNA samples (Dio-2, -3, -5, -6, -7, -8, -9, and -12) from the sample comprised of only normal 3′,5′-linkages (Dio-1). The positions of the aberrant linkages within the RNA sequence are shown in Table 1. Twelve different 21-base RNA isomers were analyzed. Except for Dio-1, each harbors at least one 2′,5′-linkage somewhere in the common sequence. For this ON sequence, samples with aberrant linkages within 5 bases of the 3′ end result in small shifts to earlier retention. Samples with aberrant linkages within 5 bases of the 5′ end show slightly larger shifts to earlier retention. Samples with isomeric linkages at positions 10–12 appear to cause significant shifts to earlier retention, while the one sample with the aberrant linkage at position 15 shifts to significantly later retention. These RNA samples are all isobaric; only a few may be resolved by reversed-phase HPLC, and none are distinguishable by single-stage mass spectrometry.

3.5. Resolution of phosphorothioate diastereoisomers

As further evidence that the DNASwift monolith is capable of separating important ON isomers that are not resolved by MS, phosphorothioate isomers were analyzed. Since replacement of the non-bridging oxygen in the phosphodiester linkage by sulfur can occur in R_p and S_p orientations, introduction of two such sites results in four diastereoisomers. Fig. 7 shows the chromatography of a sequence (as both DNA and RNA) harboring two chiral phosphorothioate linkages at specific positions in the sequence, creating diastereoisomers (see Table 1). The traces in Fig. 7 showing single peaks are those for DNA (bottom) and RNA (upper middle) with no phosphorothioate linkages. The trace with three resolved components is the doubly phosphorothioated DNA sequence, and the top trace with four resolved components is the RNA with the two phosphorothioate linkages.

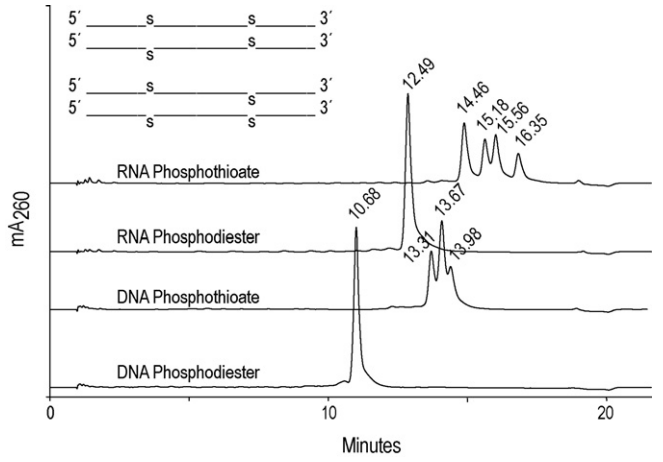

Fig. 7. Resolution of phosphorothioate diastereoisomers of DNA and RNA. Samples: 12 μg of eGFP sense strand as DNA or RNA with and without two PS linkages (see Table 1 for sequence). Gradient: 300–600 mM NaCl in 10 CV at 1.5 mL/min, pH 7 and 30 °C. Peak labels indicate retention time (min).

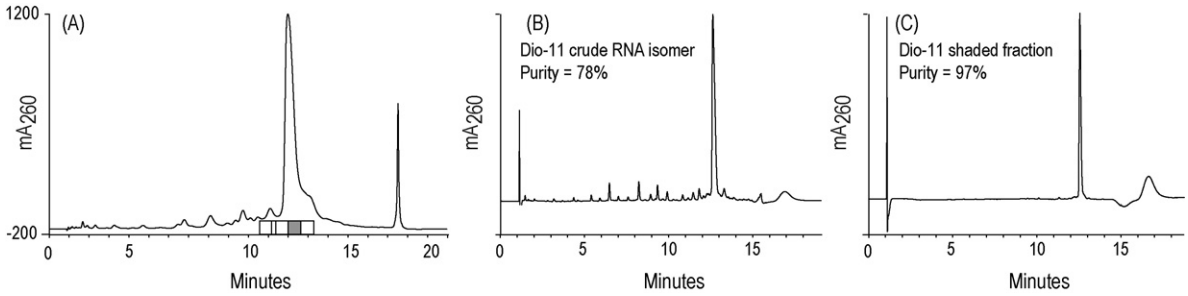

Fig. 8. Example purification of a 125 μg sample of an RNA linkage isomer. Sample: Dio-11 (see Table 1). Conditions: (A) Column DNASwift SAX-1S, Gradient: 325–525 mM NaCl in 10 CV at 1.5 mL/min, pH 7 and 30 °C, (B and C) Column: DNAPac PA200 2 mm × 250 mm, gradient: 350–650 mM NaCl in 12 min at 300 μL/min at pH 7 and 60 °C.

3.6. Sample purification and desalting

Since the DNASwift monolith is intended for oligonucleotide purification, we evaluated its ability to perform this function at low and high sample loads. One of the aberrantly linked RNA samples was purified at low sample load (125 μg, shown in Fig. 8A) using the system depicted in Scheme 1. The initial purity, as determined by DNAPac PA200 chromatography, was ~78% (Fig. 8B). After DNASwift purification, analysis of the desalted primary fraction (highlighted in A) reveals it to be ~97% pure (Fig. 8C). The fractions collected from this sample were subsequently injected onto an acclaim PA-2 cartridge to separate the desired RNA from the salt collected with it during AE chromatography. As shown in Fig. 9A, salt flows through the PA-2 cartridge, and is detected by the conductivity cell, while the ON is retained. A short step from ~0.4 to 40% MeOH elutes the purified RNA. After collection and two evaporation cycles, ESI-MS of this sample revealed the expected full-length mass of this RNA (M = 6713), with minor single and double sodium adduct formation (Fig. 9B). While this confirms excellent performance for a small-scale purification, lab-scale preparations for bioanalytical purposes often require purification of at least 1 μmol of ON.

Maximal ON yield during AE chromatography is usually obtained by overloading the column, allowing the main component of the sample (the target ON) to "displace" shorter failure sequences [28]. Based on work with a 20-base ON, we estimate the full capacity of the Mono-Q to be ~36 mg. For "Sample Self-Displacement" tests, >20% of the total capacity of the column is typically loaded [37]. In our case the test ON is a 25-base DNA with a MW of 7654. A 10 μmol synthesis of this ON produced ~31.5 mg of sample after cartridge detritylation. In order to apply 20–25% of the column capacity, we injected 2.75 μmol (8.25 mg) of the sample. Fig. 10 compares the results for the DNASwift monolith (A) and the Mono-Q (B). In Fig. 10 (A and B), one fraction from each column is shaded to indicate the elution position of a late fraction eluting just prior to the 8 μg sample peak. An example of the DNAPac analysis of the highlighted fractions in panels A and B is shown

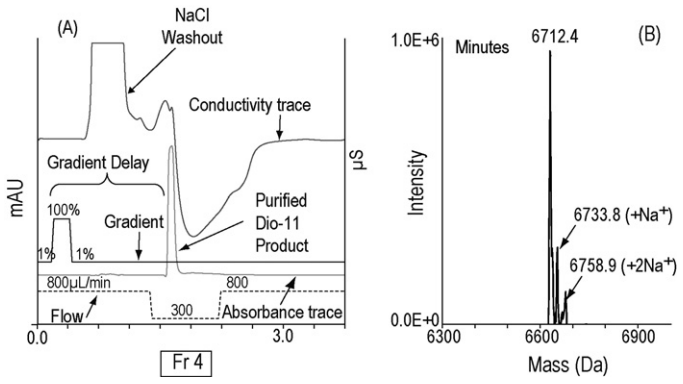

Fig. 9. Example desalting of purified 21-base RNA. (A) Sample: 85 μL of the highlighted fraction from Fig. 8. Column: Acclaim PA-2 (4.6 mm × 50 mm, equilibrated with 20 mM ammonium formate in 0.4% methanol at 800 μL/min). The salt eluted between 0.6 and 1.2 min (conductivity trace), and a 0.22 min step to 40% methanol starting at 0.16 min eluted the RNA at 1.6 min. Flow is reduced to 300 μL/min during ON elution for ESI-MS compatibility. (B) Deconvoluted ESI-mass spectrum of the desalted fraction (M = 6713).

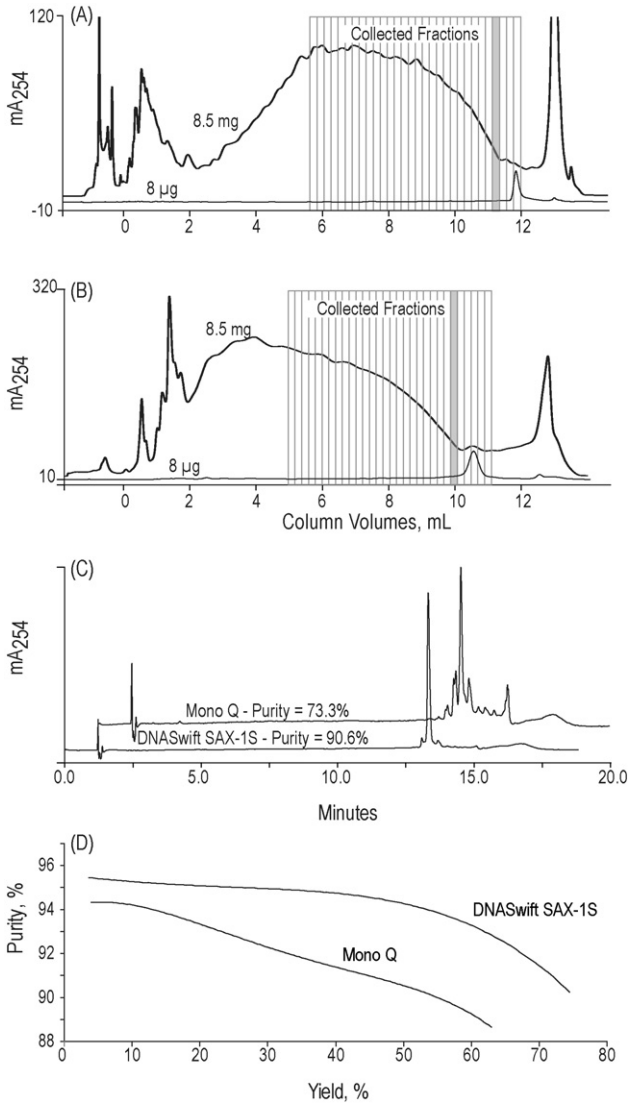

Fig. 10. Yield purity assessment using "sample self-displacement". Sample: Dx83 (see Table 1), Conditions as in Section 2. (A) DNASwift SAX-1S. (B) MONO Q. (C) Fraction analysis using the DNAPac PA200. (D) The yield vs purity results for both columns.

Table 2
The retention volumes on each column for each oligo (Dx-80 to Dx-87 from Table 1) at each of nine pH values was tabulated, and the elution volume difference between each 25-mer and its corresponding 24-mer calculated and converted into CV. This data for each ON pair can be compared to evaluate the relative selectivities of the two columns.

Column										
Mono-Q	Tr for:		pH	pH	pH	pH	pH	pH	pH	pH	pH
	Sample	24 – 25*nts*	7	8	8.5	9	9.5	10	10.5	11	12.2
	Dx80	ATG...TGA	3.67	3.90	4.02	4.18	4.54	4.96	5.36	5.60	5.70
	Dx83	CTG...TGT	3.64	3.89	4.01	4.19	4.56	5.06	5.45	5.68	5.79
	Dx85	CTG...TGG	3.69	3.93	4.07	4.23	4.61	5.5	5.56	5.78	5.90
	Dx86	ϕTG...TGA	3.61	3.86	3.98	4.14	4.55	4.99	5.38	5.60	5.71
	Dx87	CTG...TGϕ	3.65	3.90	4.02	4.19	4.61	5.07	5.45	5.66	5.77
	Retention difference										
Mono-Q	80 × 86	μL	82.5	66.0	73.5	51.0	−7.5	−33.0	−25.5	−6.0	−10.5
982 μL		**CV**	**0.08**	**0.07**	**0.07**	**0.05**	**−0.01**	**−0.03**	**−0.03**	**−0.01**	**−0.01**
	83 × 87	μL	−13.5	−15.0	−12.0	−9.0	−76.5	−6.0	0.0	31.5	33.0
		CV	**−0.01**	**−0.02**	**−0.01**	**−0.01**	**−0.08**	**−0.01**	**0.030**	**0.03**	**0.03**
	85 × 87	μL	54.0	184.5	L54.0	61.5	3.0	129.0	156.0	184.5	193.5
		CV	**0.05**	**0.06**	**0.08**	**0.06**	**0.050**	**0.13**	**0.16**	**0.19**	**0.20**
DNASwift	Tr for:		pH	pH	pH	pH	pH	pH	pH	pH	pH
	Sample		7	8	8.5	9	9.5	10	10.5	11	12.2
	Dx80	AT...GA	7.70	8.21	8.63	9.26	10.55	12.40	13.69	14.38	14.69
	Dx83	CT...GT	7.61	8.14	8.58	9.25	10.63	12.52	13.76	14.43	14.78
	Dx85	CT...GG	7.62	8.15	8.59	9.29	10.73	12.76	14.05	14.75	15.05
	Dx86	ϕT...GA	7.50	8.05	8.46	9.11	10.47	12.39	13.63	14.29	14.59
	Dx87	CT...Gϕ	7.60	8.14	8.58	9.25	10.65	14.4	13.73	14.41	14.70
	Retention difference										
DNASwift	80 × 86	μL	354.0	279.7	306.2	260.2	148.7	21.2	108.0	169.9	177.0
2474 μL		**CV**	**0.14**	**0.11**	**0.12**	**0.11**	**0.06**	**0.01**	**0.04**	**0.07**	**0.07**
	83 × 87	μL	10.6	−3.5	0.0	7.1	−31.9	−37.2	47.8	26.5	136.3
		CV	**0.00**	**0.00**	**0.00**	**0.00**	**−0.01**	**−0.02**	**0.02**	**0.01**	**0.06**
	85 × 87	μL	30.1	21.2	14.2	70.8	146.9	387.6	559.3	589.4	610.6
		CV	**0.01**	**0.01**	**0.01**	**0.03**	**0.06**	**0.16**	**0.23**	**0.24**	**0.25**

as panel C of Fig. 10. This reveals the Mono-Q fraction to be ~75% pure, while that from the DNASwift is ~90% pure. The 8.25 mg sample traces also reveal the DNASwift monolith to have somewhat greater net capacity than the Mono-Q 5 mm × 50 mm column, as separation of the failure sequences from the main sample peak is significantly greater for the DNASwift. Using the observed purity and known dilution factors for the fractions collected and evaluated on the DNAPac column, yield vs purity curves were prepared and compared in Fig. 10(D). This comparison shows that at any given purity, the DNASwift delivered higher yield than the Mono-Q, and at any given yield, the DNASwift delivered higher purity than the Mono-Q. The enhanced purity of the DNASwift-purified sample, and the overall improvement in the yield vs purity curves, likely accrue from the more effective mass transfer characteristics of the latexed monolith.

3.7. Selectivity assessment

The DNASwift monolith and the Mono-Q employ different quaternary amines to provide the strong AE functionality. An assessment of the relative selectivity of the quaternary amines used in the different columns is appropriate as they may interact differently with the phosphate backbones (and anionic nucleobases at high pH) on these columns. Table 2 details the five oligonucleotide sequences that served as test probes as described in Section 2. The selectivities of these ONs on each column at each pH are shown in Table 3.

Table 2 reveals that some ON pairs are better resolved under some conditions than others, and confirms that the DNASwift and Mono-Q offer different selectivities. For these assessments, selectivity values below 0.01 CV indicate essentially zero selectivity.

Table 3
Comparison of relative selectivities for the DNASwift SAX-1S and Mono-Q HR 5/5 columns. The selectivities for each ON pair at each pH are tabulated. Higher selectivity values are preferred.

Column												
Mono-Q	pH	7	8	8.5	9	9.5	10	10.5	11	12.2		
	Retention difference (CV)											
	80 × 86	0.08	0.07	0.07	0.05	−0.01	−0.03	−0.03	−0.01	−0.01		
982 μL	83 × 87	−0.01	−0.02	−0.01	−0.01	−0.08	−0.01	0.030	0.03	0.03		
	85 × 87	0.05	0.06	0.08	0.06	0.050	0.13	0.16	0.19	0.20		
DNASwift												
	Retention difference (CV)											
	80 × 86	0.14	0.11	0.12	0.11	0.06	0.01	0.04	0.07	0.07		
	83 × 87	0.00	0.00	0.00	0.00	−0.01	−0.02	0.02	0.01	0.06		
	85 × 87	0.01	0.01	0.01	0.03	0.06	0.16	0.23	0.24	0.25		
	Relative selectivity										Sums	Frequency
DNASwift > MQ		1	1	1	1	2	1	3	2	3	15	56%
MQ > DNASwift		1	1	1	1	0	0	0	1	0	5	19%
MQ–DNASwift		1	1	1	1	1	2	0	0	0	7	26%
	Elution order inversions											
MQ		1	1	1	1	3	2	2	1	1	13	48%
DNASwift		1	2	2	1	1	2	0	0	0	9	33%

Based on this data, the relative advantage for each column is tabulated (in Table 3) under the heading: "Relative Selectivity". These entries reveal that the Mono-Q offers higher selectivity than the DNASwift in 5 of 27 cases (19%). Conversely, the DNASwift offers higher selectivity in 16 of 27 cases (59%). Selectivity should be both positive and as high as possible. The bottom two rows of Table 3 indicate the number of zero, or negative selectivity values for each column under each condition with this set of ONs. Overall the Mono-Q exhibits zero or negative selectivities in 13 of 27 cases (48%), while the DNASwift does so in 6 of 27 cases (22%), less than half that of the Mono-Q.

4. Conclusions

We have prepared a new surface-functionalized monolith for lab-scale purification of nucleic acids. The new column combines several attributes known to promote convective (rather than diffusive) mass transfer, and employs nanobead chemistry (from the DNAPac columns) optimized for nucleic acid separations. This phase permits flows to 3 mL/min in a 5 mm × 150 mm format with minimal loss of resolution when compared to lower flow rates. The nanobead coating improves selectivity and helps control hydrophobic interactions that contribute to tailing and band broadening compared to porous bead phases. The nanobead size and porosity is engineered to provide a substantial increase in ON capacity over other pellicular phases and is competitive with fully porous packed bed columns. The DNASwift exhibits increased retention and improved peak shape with increasing temperatures, characteristic of AE columns. In addition, the monolith showed separation of derivatized ONs from their unlabeled parents, and the ability to resolve several isobaric RNA linkage isomers, as well as phosphorothioate diastereoisomers in DNA and RNA. Since selectivity tests for certain ON pairs revealed elution of a 24-base ON after that of a 25 base ON, we also demonstrated options for controlling elution order with changes to mobile-phase pH and salt-form. The latex-coated monolith accommodates oligonucleotide sample self-displacement purification of at least 8.25 mg of oligonucleotide in a single chromatographic process: the resulting purity (>90%) at 75% yield represents an 18% yield improvement over that of the Mono-Q bead-based column. The DNASwift monolith offers performance superior in resolution, peak capacity, pressure stability, and selectivity (as measured by $n, n-1$ resolution and frequency of elution order inversions) to the benchmark porous anion-exchange column, it may be run at elevated pH, and can be cleaned in place with a combination of high salt and high pH (1 M NaCl and NaOH). We described a means to couple anion-exchange purification with desalting to automatically prepare purified ONs for ESI-MS and other salt-sensitive applications.

The new monolith and desalting method should find utility for purification and critical analyses of ss- and ds-DNA and RNA, aptamers, and nucleic acids that may harbor isobaric linkage isomers, such as phosphorothioate diastereoisomers and similar isobaric ON variants.

Disclosure statement

The authors are employed by Dionex Corporation, and may be minor stockholders. To the extent that this publication may alter Dionex stock price, the authors may benefit, or suffer minor financial change. Dionex holds registered patents on the technologies applied to the DNASwift column (US 5453185, US 5936003 and US 7303671), but none of the authors are remunerated based on publications. We believe that publication of this work will help enterprises involved in research and development of oligonucleotide therapeutics and diagnostics more fully evaluate and characterize their products. We believe this will result in safer, more effective therapeutic and diagnostic products. Such efforts are not part of Dionex corporate focus.

Acknowledgements

Yury Agroskin, Doug Jamieson, Emily Hilder and Jim Maher for their contributions towards completion of this project.

References

[1] P.S. Miller, L.T. Braiterman, P.O.P. Ts'o, Biochemistry 16 (1977) 1988.
[2] P.C. Zamecnik, M.L. Stephenson, Proc. Natl. Acad. Sci. U.S.A. 75 (1978) 280.
[3] M. Matsukura, K. Shinozuka, G. Zon, H. Mitsuya, M. Reitz, J.S. Cohen, S. Broder, Proc. Natl. Acad. Sci. U.S.A. 84 (1987) 7706.
[4] S.M. Gryaznov, R.L. Letsinger, Nucleic Acids Res. 20 (1992) 3403.
[5] D.V. Morrissey, J.A. Lockridge, L. Shaw, K. Blanchard, K. Jensen, W. Breen, K. Hartsough, L. Machemer, S. Radka, V. Jadhav, N. Vaish, S. Zinnen, C. Vargeese, K. Bowman, C.S. Schaffer, L.B. Jeffs, A. Judge, I. MacLachlan, B. Polisky, Nat. Biotechnol. 23 (2005) 1002.
[6] Y. Shiba, H. Masuda, N. Watanabe, T. Ego, K. Takagaki, K. Ishiyama, T. Ohgi, J. Yano, Nucleic Acids Res. 35 (2007) 3287.
[7] X. Yang, R.P. Hodge, B.A. Luxon, R. Shope, D.G. Gorenstein, Anal. Biochem. 306 (2002) 92.
[8] F. Wincott, A. DiRenzo, C. Shaffer, S. Grimm, D. Tracz, C. Workman, D. Sweedler, C. Gonzalez, S. Scaringe, N. Usman, Nucleic Acids Res. 23 (1995) 2677.
[9] J.R. Thayer, V. Barreto, S. Rao, C. Pohl, Anal. Biochem. 338 (2005) 39.
[10] Y.Z. Xu, P.F. Swann, Anal. Biochem. 204 (1992) 185.
[11] T.P. Shields, E. Mollova, L. Ste Marie, M.R. Hansen, A. Pardi, RNA 5 (1999) 1259.
[12] C.A. Pohl, J.R. Stillian, P.E. Jackson, J. Chromatogr. A 789 (1997) 29.
[13] A.J. Bourque, A.S. Cohen, J. Chromatogr. B 662 (1994) 343.
[14] K. Srinivasan, P. Zakaria, N. Avdalovic, C.A. Pohl, P.R. Haddad, Ion exchange particle-bound flow-through porous monolith, Patent Number 7303671 B2, 12-4-2007.
[15] R.W. Slingsby, C.A. Pohl, J. Chromatogr. 458 (1988) 241.
[16] F. Svec, J.M.J. Frechet, Anal. Chem. 64 (2002) 820.
[17] E.G. Vlakh, T.B. Tennikova, J. Chromatogr. A 1216 (2009) 2637.
[18] C.G. Huber, P.J. Oefner, E. Preuss, G.K. Bonn, Nucleic Acids Res. 21 (1993) 1061.
[19] D. Sýkora, F. Svec, J.M.J. Fréchet, J. Chromatogr. A 852 (1999) 297.
[20] J.P. Hutchinson, E.F. Hilder, M. Macka, N. Avdalovic, P.R. Haddad, J. Chromatogr. A 1109 (2006) 10.
[21] P. Zakaria, J.P. Hutchinson, N. Avdalovic, Y. Liu, P.R. Haddad, Anal. Chem. 77 (2005) 417.
[22] E.F. Hilder, F. Svec, J.M.J. Fréchet, J. Chromatogr. A 1053 (2004) 101.
[23] E.C. Peters, M. Petro, F. Svec, J.M.J. Frechet, Anal. Chem. 70 (1998) 2288.
[24] F. Svec, C.G. Huber, Anal. Chem. 78 (2006) 2100.
[25] J.R. Thayer, S. Rao, N. Puri, C.A. Burnett, M. Young, Anal. Biochem. 361 (2007) 132.
[26] J.R. Thayer, S. Rao, N. S Puri, S. Beaucage (Eds.), Detection of Aberrant 2′–5′ Linkages in RNA by Anion Exchange, Curr. Protoc. Nucleic Acid Chem, John Wiley & Sons, Inc., 2008, pp. 10.13.1–10.13.11.
[27] J.K. Chen, R.G. Schultz, D.H. Lloyd, S.M. Gryaznov, Nucleic Acids Res. 23 (1995) 2661.
[28] J.R. Thayer, R.M. McCormick, N. Avdalovic, Methods Enzymol. 271 (1996) 147.
[29] B.J. Bergot, W. Egan, J. Chromatogr. 599 (1992) 35.
[30] C. Crean, Y. Uvaydov, N.E. Geacintov, V. Shafirovich, Nucleic Acids Res. 36 (2008) 742.
[31] H. Yang, S.L. Lam, FEBS Lett. 583 (2009) 1548.
[32] H. Stansfield, B. Kulczewski, K. Lybrand, E. Jamieson, J. Biol. Inorg. Chem. 14 (2009) 193.
[33] Y. Jung, Y. Mikata, S.J. Lippard, J. Biol. Chem. 276 (2001) 43589.
[34] J. Gallego, D. Loakes, Nucleic Acids Res. 35 (2007) 2904.
[35] G.P.G. Grant, A. Popova, P.Z. Qin, Biochem. Biophys. Res. Commun. 371 (2008) 451.
[36] A.Y. Tsygankov, Y. Motorin, A.D. Wolfson, D.B. Kirpotin, A.F. Orlovsky, J. Chromatogr. 465 (1989) 325.
[37] R.R. Deshmukh, W.E. Leitch II, D.L. Cole, J. Chromatogr. A 806 (1998) 77.